Title

Dysregulated NF-κB–Dependent ICOSL Expression in Human Dendritic Cell Vaccines Impairs T-cell Responses in Patients with Melanoma

Permalink

https://escholarship.org/uc/item/16w5c93b

Journal

Cancer Immunology Research, 8(12)

ISSN

2326-6066

Authors

Maurer, Deena M
Adamik, Juraj
Santos, Patricia M
et al.

Publication Date

2020-12-01

DOI

10.1158/2326-6066.cir-20-0274

Peer reviewed

Dysregulated NFκB-dependent ICOSL Expression in Human Dendritic Cell Vaccines Impairs T-cell Responses in Melanoma Patients

Deena M. Maurer[1], Juraj Adamik[3], Patricia M. Santos[2], Jian Shi[2], Michael R. Shurin[4], John M. Kirkwood[2], Walter J. Storkus[4,5,6], Lisa H. Butterfield[3]

[1]Department of Immunology, University of Pittsburgh, Pittsburgh, PA 15213

[2]UPMC Hillman Cancer Center, Department of Medicine, University of Pittsburgh, Pittsburgh, PA 15213

[3]Parker Institute for Cancer Immunotherapy, and University of California San Francisco, Microbiology and Immunology, San Francisco, CA 94129

[4]Department of Pathology, University of Pittsburgh, Pittsburgh, PA 15213

[5]Department of Dermatology, University of Pittsburgh, Pittsburgh, PA 15213

[6]Department of Bioengineering, University of Pittsburgh, Pittsburgh, PA 15213

Abstract

Therapeutic cancer vaccines targeting melanoma-associated antigens are commonly immunogenic, but are rarely effective in promoting objective clinical responses. To identify critical molecules for activation of effective antitumor immunity, we have profiled autologous dendritic cell (DC) vaccines used to treat 35 patients with melanoma. We showed that checkpoint molecules induced by *ex vivo* maturation correlated with *in vivo* DC vaccine activity. melanoma patient DCs had reduced expression of cell surface ICOSL and had defective intrinsic NF-kB signaling. ChIP assays revealed NF-kB-dependent transcriptional regulation of ICOSL expression by DCs. Blockade of ICOSL on DCs reduced priming of antigen-specific CD8$^+$ and CD4$^+$ T cells from naïve donors *in vitro*. Concentration of extracellular/soluble ICOSL released from vaccine DCs positively correlated with patient clinical outcomes, which we showed to be partially regulated by ADAM10/17 sheddase activity. These data point to the critical role of canonical NF-kB signaling, the regulation of matrix metalloproteinases, and DC-derived ICOSL in the specific priming of cognate T-cell responses in the cancer setting. This study supports the implementation of targeted strategies to augment these pathways for improved immunotherapeutic outcomes in cancer patients.

Keywords

ICOSL; cancer vaccine; NFκB Signaling; dendritic cells; melanoma

Corresponding author: Lisa H. Butterfield, Ph.D., Parker Institute for Cancer Immunotherapy, 1 Letterman Drive, Suite D3500, San Francisco, CA 94129, Phone: 628-899-7598, lbutterfield@parkerici.org.

Introduction

Melanoma is the leading cause of skin cancer-related deaths in the United States and the incidence rate of the disease continues to rise annually (1). Immune checkpoint blockade (anti-CTLA-4 and anti-PD-1/anti-PD-L1) therapies have shown durable therapeutic efficacy (2–5). Nonetheless, only a minority of patients display durable objective clinical benefit (2–5). Cancer vaccines based on dendritic cells (DCs) provide three essential signals (antigen presentation, costimulation, and proinflammatory cytokine production) required to initiate Type-1 adaptive immune responses (6–10). However, clinical response rates for DC vaccines in metastatic cancer patients remain low (i.e. 5–10%), indicating that critical pathways for activating effective immunity remain unknown (11).

To improve outcomes, we developed a genetically engineered DC-based vaccine using a recombinant adenovirus coordinately expressing three shared melanoma antigens: tyrosinase, MART-1, and MAGE-A6 (TMM2) to promote an expanded antitumor CD4$^+$ and CD8$^+$ T-cell repertoire. Monocyte-derived DCs were first matured with recombinant human (rh)IFNγ+lipopolysaccharide (LPS), and then transduced with recombinant adenovirus (AdVTMM2) before administration to patients (n=35) 3x via bi-weekly intradermal injections. Given clinical outcome data from these patients and our previous findings that vaccine bioefficacy did not correlate with administered DC expression of commonly tested costimulatory molecules (CD80, CD86) or IL12p70 (12), in the current study, we performed gene and protein expression profiling to identify key biomarkers associated with *in vivo* DC immunogenicity and positive clinical response to DC-based vaccination. We report that cell surface expression of Inducible T-cell Costimulator Ligand (ICOSL) is selectively reduced on DCs from melanoma patients and partially regulated by canonical NF-κB signaling, resulting in a vaccine that is suboptimal for T-cell (cross)priming. We further showed that concentration of soluble ICOSL (sICOSL) positively correlated with production of Th1 immune chemokines, objective clinical response rates, and overall survival in advanced-staged melanoma patients. We also showed that sICOSL was partially regulated by ADAM10/17 sheddase activity on monocyte-derived DCs. These data suggest that targeted manipulation of patient-derived DCs to improve ICOSL expression may improve therapeutic T-cell responses and treatment outcomes in cancer patients.

Methods

Patients and vaccination strategy

Thirty-five late staged melanoma patients were enrolled in the phase I clinical trial (12). Three patients were treatment naïve, whereas the others had previously received standard of care (IFNα and/or IL2) or checkpoint blockade therapies (ipilimumab and/or pembrolizumab). A detailed patient demographic table is located in the supplementary figures (Supplementary Table S1). For detailed information regarding the clinical trial, please refer to the previously published trial report (12).

AdVTMM2 Virus

The replication-deficient E1/E3-deleted Ad5 TMM2 virus coordinately encoding full-length cDNAs for tyrosinase, MART-1, and MAGE-A6 used in this study was manufactured as previously described (13). DCs, generation described below, were harvested 24hrs. post-maturation and transduced with the adenovirus at an MOI of 400. CellGenix GMP DC Medium, serum free (CellGenix, #20801–0500) was used for the transduction. DCs and the AdVTMM2 virus in CellGenix medium were incubated for 3hrs. at 37°C, and then washed with PBS.

DC generation from cryopreserved monocytes

Patient and healthy donor (HD) PBMCs were isolated by leukapheresis and elutriation (12). Fractioned cells were cryopreserved using freezing cryovials, 1.8 mL internal thread (Nunc Cat. No. 368632). Freezing media contained 20% DMSO in Dulbecco's Modified Eagle Medium (Gibco/Invitrogen, Catalog #11885), complete media [20% heat-Inactivated Fetal Bovine Serum (FBS) (Gibco/Invitrogen, Catalog #16000), 1% L-glutamine (Gibco/Invitrogen, Catalog # 25030), and 1% pen/step (Gibco/Invitrogen, Catalog #15140)]. Monocyte-enriched fractions were thawed using RPMI (Gibco/Invitrogen, Catalog #11875–085) complete media [1% pen/strep, 1% L-glutamine, 10% FBS Heat-Inactivated Serum (Gibco-Invitrogen, Catalog #16000–044), and 0.5% DNase (Sigma, Catalog # DN-25)]. Cells were centrifuged at 1200 RPM (31 x g) for 10 minutes and then washed twice with PBS. Cells were counted, analyzed for viability using Trypan Blue Stain 0.4% (Gibco, Catalog #15250–061), and plated at 1×10^6/mL in CellGenix DC medium, serum free (CellGenix, Catalog #20801–0500). To culture patient DCs for checkpoint and costimulatory protein surface molecule expression, the conditions were identical to Standard Operating Procedures used in the clinical trial [Cell Genix with GM-CSF (1000 U/mL; Genzyme and Sanofi) and IL4 (1000 U/mL; Cell Genix)](12). For all other experiments, research grade reagents were used [AIMV Media (Gibco-Invitrogen) with GM-CSF (800U/mL; Genzyme and Sanofi) and of IL4 (500 U/mL; Cell Genix)]. On day 5, immature DCs (iDCs) were matured by addition of rhIFNγ (1000 U/mL; Actimmune and R&D Systems) + LPS (250 ng/mL; Sigma-Aldrich) in CellGenix DC medium, serum free for 24hrs. (mDCs). Matured DCs were transduced with clinical-grade TMM2 adenovirus at a MOI of 400 for 3hrs. at 37°C, and then washed with PBS. Cells were rested overnight in DC media with IL4 and GM-CSF (1000 U/mL; AdVTMM2/DC).

Cell surface and intracellular flow cytometry

DCs were harvested, washed twice with PBS, prior to counting and assessment of viability by trypan blue dye exclusion. Viability was validated by the use of Zombie Aqua Viability Dye (BioLengend #423101). The viability dye was used per manufacturer's instructions. Cells were washed with FACS buffer (2% BSA, and 0.02% NaN_3 in PBS). Fc blocking was done using 5% Human Antibody Serum (Corning) for 25 minutes at 4°C. Antibody staining was performed for 20 minutes at 4°C. Cells were washed and fixed using 2% paraformaldehyde for 30 minutes at room temperature (RT) or overnight at 4°C. For intracellular staining, the cells were permeabilized (0.1% saponin in FACS buffer) for 30 minutes at RT and then stained for 45 minutes at RT. Flow cytometry was performed using

the BD LSR Fortessa II (BD Biosciences), with data analyzed using FlowJo v10 software. DCs were identified as HLA-DR$^+$CD86$^+$ double-positive cells. Mean fluorescence intensity (MFI) or positive frequencies were determined after correcting for background staining using an isotype control. All isotype antibodies used and vendor information is the next sub-section. A 2% threshold was used to determine positive staining (Supplementary Fig. S1A–E). MFI and positive frequency values were validated using DCs from two vaccinated patients. Validation thresholds were set at 10% change.

Antibodies

The following antibodies were used for assessment of costimulatory and checkpoint molecule expression on DC subsets: FITC Mouse Anti-Human HLA-DR (BD Biosciences Catalog#555811), PE-Cy7 Mouse Anti-Human CD86 (BD Biosciences Catalog#561128), BV 421 Mouse Anti-Human PD-L1 (BioLegend Catalog#329714), BV 711 Mouse Anti-Human PD-L2 (BD Biosciences Catalog#564258), BV711 Mouse IgG1, κ Isotype Control (Biosciences Catalog#563044), BV786 Mouse Anti-Human CTLA-4 (BD Biosciences Catalog#563931), BV786 Mouse IgG2a, κ Isotype Control (BD Biosciences Catalog#563732), ICOSL (BD Biosciences Catalog#564276), and BV 421 Mouse IgG2b, κ Isotype Ctrl Antibody (BioLegend Catalog#400342). The following antibodies were used for intracellular staining of NF-κB molecules: NF-κB p65 (D14E12) Rabbit mAb (Alexa Fluor® 647 Conjugate; Cell Signaling #8801S), Phospho-NF-κB p65 (Ser536) Rabbit mAb (PE Conjugate; Cell Signaling #5733S), Rabbit IgG Isotype Control (Alexa Fluor® 647 Conjugate; Cell Signaling # 3452S), Rabbit (DA1E) mAb IgG XP® Isotype Control (PE Conjugate; Cell Signaling #5742). The following antibodies were used for ImageStream Analysis: NF-κB p65 (D14E12) Rabbit mAb (Alexa Fluor® 647 Conjugate; Cell Signaling #8801S), PE Mouse Anti-IκBα (Clone 25/IkBa/MAD-3; BD Biosciences #560818), DAPI Solution (BD Biosciences #564907). ImageStream analysis was done using the ImageStreamX Mark II (Amnis) and analyzed using IDEAS (Image Data Exploration and Analysis Software, Amnis). The following antibodies were used for ICOSL functional assays: FITC Mouse Anti-Human CD3 (HIT3α; BD Biosciences #555339), APC-Cy7 Mouse Anti-Human CD4 (RPA-T4; BD Biosciences #557871), PE-Cy7 Mouse Anti-Human CD8 (RPA-T8; BD Biosciences #557746), PE Mouse Anti-Human CD107a (H4A3; BD Biosciences #555801), PE Mouse IgG1, κ Isotype Control (MOPC-21; BD Biosciences #559320), CD275 (B7-H2) Monoclonal Antibody (MIH12; eBioscience #16-5889-82), and Mouse IgG1 kappa Isotype Control (eBioscience#16-4714-82).

ICOSL *in vitro* function assays

HD PBMCs were purified by Ficoll-hypaque gradient centrifugation (GE Healthcare - #17144022). CD14$^+$ monocytes were selected using CD14 microbeads (Miltenyi Biotec #130-050-201), and DCs were generated as outlined above. Autologous CD14^{neg} cells were cryopreserved in 10% (v/v) DMSO (Protide Pharmaceuticals, Inc., Catalog #PP1400)+ 90% (v/v) human serum(Gemini Bio Products, Catalog #100–512) for later use. On Day 5, immature DC cultures were split into two fractions: half of the cells were frozen for future use and the other half were matured as outlined above. Following 24-hr. maturation, DCs were pulsed with a CMV pp65 peptide pool (15-mer peptides, with 11 amino acid overlap; total 2 ng per peptide added; Miltenyi Biotec #130-093-435) for 2hrs. at 37°C. The cells

were then washed and split into three groups: negative control (mDCs alone), IgG-treated control (10 µg/mL; eBioscience, Catalog # 16-4714-82), or an anti-ICOSL-treated group (10 µg/mL; eBioscience, Catalog #16-5889-82). DCs were incubated with nothing or the respective antibodies for 3hrs. at 37°C in AIMV media. Following incubation, DCs were cocultured with autologous CD14^{neg} (i.e. T cell-enriched) cells (at a 1:10 ratio) in AIMV media and 5% human serum for 7 days. rhIL7 (10 ng/mL final concentration; Sigma-Aldrich) was added to the coculture on day 1, with rhIL15 (10 ng/mL final concentration; Sigma-Aldrich, Catalog # IL013) added on day 4. On day 7 of the coculture, activated T cells were harvested, counted, and a viability test performed using trypan blue. Cryopreserved autologous iDCs were thawed, pulsed with the CMV peptides, (2 ng per peptide added, please see above) and cocultured with activated autologous T cells (at a 1:10 ratio) for seven days. Responder T cells were restimulated in an identical manner, with rhIL15 added every 2–3 days (10 ng/mL final concentration).

Seven days after boosting, T-cell function was assessed. T cells were harvested, counted, and each group (T cells pulsed with mDC control, IgG-treated control, or anti-ICOSL-treated DCs) was split into four simulation groups: No stimulation (responder T cells alone), Negative Control (Non-pulsed DCs + responder T cells (1:10 ratio), Positive Control (T cells stimulated with PMA(20ng/mL; Sigma-Aldrich, Catalog #P8139) and ionomycin(1 µg/mL; Sigma-Aldrich, Catalog #I0634), and CMV peptide-pulsed (CMV pulsed DCs + responder T cells (at a 1:10 ratio). Cells were stimulated for 5hrs. at 37°C. For each condition, a CD107a antibody or an isotype control was added, and CD107a expression was determined using flow cytometry. MFI was determined after subtracting isotype control values from the stained samples. A 2% threshold was used to determine positive staining, compared to isotype controls. CD107a MFI values for the negative control were subtracted from the MFI of the CMV experimental group to determine true CD107a staining. Because CD8 and CD4 molecules were downregulated on the T-cell surface for several days after antigen-specific activation, CD3^{+}CD4^{dim} or CD3^{+}CD8^{dim} cells were gated for subsequent assessment of CD107a expression. A Zombie Aqua Dye was used to confirm viability (Supplementary Fig. S1F–I). Culture supernatants were collected on day 7 (time of boost), day 9 (2 days after boosting), day 11 (4 days after boosting), and day 16 (7 days after boosting) for analysis of secreted products in ELISA or Luminex assays.

Soluble ICOSL ELISA

Soluble ICOSL concentrations were determined using the Human B7-H2 Duo Kit ELISA (R&D #DY165–05) and the DuoSet ELISA Ancillary Reagent Kit 2 (R&D #DY008). R&D company protocols were followed. Cell culture supernatants were diluted at either a 1:5 ratio (AdV/DC supernatants) or 1:2 ratio (mDC supernatants). All standards and samples were run in triplicate. Absorbance readings were read using the Spectramax 340PC Microplate Reader (Molecular Devices). The concentrations of the standard controls were used to generate a standard curve using SoftMax Pro Software (Version 4). Sample concentrations were determined by interpolating absorbance readings of samples to the generated standard curve.

Luminex

A Human Checkpoint 14-plex (Thermo-Fisher Procarta Plex) was used for detection of checkpoint and costimulatory molecules in culture supernatants. A custom 2-Plex (Thermo-Fisher Procarta Plex) for granzyme-B and IFNγ was used for detection of granzyme-B. Immune Monitoring 65-Plex (Thermo-Fisher Procarta Plex) was used for the detection of chemokine and cytokine secretion in DC culture supernatants. Serum was diluted 1:1 per manufacturer's instructions, analyzed in a BioRad BioPlex System 100. Experimental data was analyzed using five-parametric curve fitting and assay controls included kit standards and multiplex QC controls (R & D Systems).

Detection of IgM and IgG antibodies against CMV in HD serum

The Bioplex 2200 System and Infectious Disease Panel (BioRad) were used to detect antibodies against CMV in HD serum collected from whole blood. Testing was performed according to the manufacturer's instructions using the BioPlex ToRC IgG and IgM kits on the BioPlex 2200 analyzer (Bio-Rad). The BioPlex used a total input volume of 5 μL serum or plasma for the analytes. Following flow cytometric analysis, the data were initially calculated in relative fluorescence intensity (RFI) and were then converted to a fluorescence ratio (FR) using the internal standard bead. The FR was compared to an assay-specific calibration curve to determine analyte concentration in antibody index units (AI). The interpretive criteria were established by the manufacturer, and results were defined as negative (0.8 AI), equivocal (0.9 to 1.0 AI), or positive (1.1 AI). The BioPlex 2200 Software Version 4.2. was used for all calculations.

NF-κB inhibition

Day 5 iDCs were generated from HD and divided into the following groups: 1) iDC control (untreated), 2) stimulated with rhIFNγ + LPS, 3) DMSO control (rhIFNγ + LPS + DMSO), and 4) NFκBi (rhIFNγ + LPS + parthenolide, 15 μM; Abcam #120849)). On day 5, iDCs were incubated with the above reagents for 15 minutes at 37°C in DC media. After stimulation and/or blocking, total p65, phospho-p65, and ICOSL protein surface expression was measured by flow cytometry. A Zombie Aqua Dye was used to confirm viability.

Chromatin immunoprecipitation (ChIP) assay

Chromatin from mDCs was analyzed using a modification of the ChIP Cell Signaling technology protocol (9005) using Micrococcal Nuclease (CST, 10011) and Magna ChIP Protein A+G Beads (16–663, Millipore). An NF-κB antibody (Santa Cruz, sc-8008) was used for ChIP. Modified step included DNA elution, which was carried out using GeneJET PCR Purification Kit (Thermo-Fisher, K0702). Aliquots for input and non-specific IgG control samples were included with each experiment. Fold-enrichment was calculated based on Ct as 2(Ct), where Ct = (CtInput – CtIP). The IgG Ct was subtracted from the specific antibody Ct to generate Ct = (Ctspecific Ab – CtIgG). ChIP-qPCR primers used: *ICOSLG* Forward – GCTTCCCAGGGCACCTAC; *ICOSLG* Reverse- CTCCGGAAAGTTCGGCTCT; *ICOSLG* (Exon) Forward – GAAGGAAGTCAGAGCGATGG; *ICOSLG* (Exon) Reverse – GGAGCTGTTCTGTGGGATGT; *TNFα NF-κB Site* Forward –

TGAGCTCATGGGTTTCTCCACCAA; *TNFα NF-κB Site* Reverse –
ACAACTGCCTTTATATGTCCCTGG; *TNFα* (Exon) Forward –
TGGGTGAAAGATGTGCGCTGATAG; *TNFα* (Exon) Reverse-
TTGCCACATCTCTTTCTGCATCCC

ADAM10/17 inhibition

Day 5 iDCs were generated from HDs and divided into the following groups: 1) iDC
baseline control, 2) mDC (rhIFNγ + LPS 24hrs.), and 3) ADAM10/17i [(rhIFNγ + LPS +
Tapi-2; 20 μM, Tocris #6013)]. On day 5, iDCs were matured using rhIFNγ + LPS alone or
in the presence of Tapi-2 for 24hrs. Tapi-2 has been shown to inhibit the sheddase activity
for ADAM10, ADAM17, and other metalloproteases (14,15). Cell culture supernatants were
collected post-maturation for observation of sICOSL. Surface ICOSL was assessed by flow
cytometry. A Zombie Aqua Dye was used to confirm viability. Viability of the DCs averaged
73% using 20 μM of the inhibitor.

Transcriptional analysis of costimulatory/checkpoint molecules

RNA from DC preparations was collected using the All Prep RNA/Protein kit
(Qiagen#80404). cDNA was synthesized using the qScript cDNA Synthesis Kit (Quantabio).
cDNA synthesis used between 25–37.5 ng/uL RNA input. QPCR was performed using
standard Taqman primers (listed below) and the Express qPCR supermix (Thermo Fisher
#1178501K). The following primers were used: *CD274* (Hs00204257_m1), *CTLA4*
(Hs00175480_m1), and *ICOSLG* (Hs00391287_m1). *HPRT1* (Hs99999909_m1) was used
as a housekeeping control. All experiments were done in triplicates using the StepOne Plus
Real-time PCR System (Applied Biosystems). Gene expression was calculated and
normalized to the *HPRT1* endogenous control using the Livak and Schmittgen method (2
$^{– \Delta\Delta CT}$).

DC microarrays

Patient-derived immature, matured, and adenovirally-transduced DCs were harvested (as
described above), washed with PBS, and centrifuged at 1200 RPM (30 x g). Cell pellets
were collected and resuspended in RNAlater (Invitrogen; Catalog #AM7021), placed at 4°C
overnight, and then moved to −80°C for storage. RNA was analyzed using HUGENE 2.0 ST
gene arrays (Affymetrix)(GSE157738). Human microarray and qPCR data from patients
confirmed *in vitro* adenovirus transduction based on increased expression of transcripts for
tyrosinase, MART-1 and MAGE-A6, as well as the adenoviral hexon gene product
(Supplementary Fig. S2A–B). A publicly-available HD DC dataset was used as for
comparison (GSE111581)(16) using the same maturation protocol in preparing DC from
both patients and HDs. Patient and HD microarray data and differential gene expression was
analyzed using R statistical packages, limma (Version 3.38.3) and oligo (Version 3.9)
(17,18). The Robust Multi-Average (RMA) method was used to normalize the data, and the
Benjamin-Hochberg Procedure was used to adjust for type-1 error rate. Ingenuity Pathway
Analysis software (QIAGEN Bioinformatics) was used for comparative analysis between
patient and HD datasets. The patient and HD datasets used different gene array platforms,
hence pathway analysis focused on opposing trends that might underlie differential gene
profiling. Pathways and/or genes with the same directional pattern (activation or inhibition)

were not prioritized for further consideration. Significant adjusted p value and log fold-change thresholds were set at 0.05 and 1.2, respectively.

Clinical outcome comparison groups

For all analyses, clinical outcome groups were defined based on time to progression (Supplementary Table S1) using RECIST 1.1. Patients who showed tumor regression (PR), remained stable (SD), or were considered "No Evidence of Disease" (NED) at enrollment and remained NED for at least eighteen months (NED1) were considered to have "favorable/good outcomes" (i.e. good). Patients were classified as "No Evidence of Disease" if they previous had measurable disease which was treated, but did not have measurable disease at time of enrollment. Patients who had early tumor progression or were considered "No Evidence of Disease" at enrollment, but remained NED for less than eighteen months (NED2) were considered to have "bad outcomes" (i.e. bad). Eighteen months was chosen for the cutoff because patients who remained NED for at least eighteen months were suggested to have been clinically impacted by the vaccine.

Statistical analysis

Based on data distribution, *t*-tests or Wilcoxon rank-sum test were used for most of the analyses. The Shapiro-Wilk test was used to asses data normality. When appropriate, one-way ANOVA or Kruskal-Wallis one-way ANOVA tests were performed. To test for multiple comparisons, a Dunnett multiple comparison or Tukey comparison test was used. Pearson or Spearman's correlation coefficients and linear regression models were calculated to determine associations present. Kaplan-Meier (KM) curves and Cox proportional-hazards modeling were carried out using the R packages survival (version 3.1–8) and survminer (version 0.4.6). Associations between *ICOSLG* expression and CD8+ T-cell infiltrates across cutaneous melanoma tumors were evaluated using publicly available software Timer 2.0. (http://timer.cistrome.org/). P values are represented as *p 0.05, **p 0.01, ***p 0.001, ****p 0.0001. Graphs and statistical calculations were generated using the R package ggplot2 (Version 3.1.1) and GraphPad Prism v7.

Results

Conventional DC phenotype does not correlate with clinical outcome or T-cell responsiveness

Expression of HLA-DR, CD11c, CD40, CD80, CD83, CD86, and CCR7 on vaccine DC did not correlate with immune or clinical outcomes (Supplementary Fig. S3A). Cox regression analysis revealed that these markers were not prognostic factors for overall survival (OS) or progression-free survival (PFS)(Supplementary Table S2). Unlike some prior reports (19,20), DC production of IL12p70 (either spontaneous or after CD40L-induced activation), an essential cytokine for promotion of type-1 immunity, also failed to correlate with immune or clinical outcomes (Supplementary Fig. S3B–C). This was also the case for DC production of the immunoregulatory molecule IL10 (Supplementary Fig. S3B–C). RNA expression of most of these cell surface and secreted molecules increased with DC maturation, as expected, but RNA expression also failed to correlate with objective clinical outcomes (Supplementary Fig. S3D–E).

DCs exhibit increased cell surface expression of PD-L1, PD-L2, and CTLA-4 post-maturation

To identify critical molecules important for promotion of antitumor T-cell responses, eleven different costimulatory and immune checkpoint molecules previously suggested to be important for antigen presentation and T-cell activation were evaluated. Protein expression of PD-1, PDL-1, PD-L2, CTLA-4, LAG-3, Galectin-9, OX40L, CD70, B7-H4, B7-H5, and ICOSL were assessed on iDCs, mDCs, and AdVTMM2/DC from melanoma patients and HDs. Surface protein expression of 8/11 molecules (PD-1, PDL-1, PD-L2, CTLA-4, LAG-3, B7-H4, B7-H5, and ICOSL) was validated on DCs from two vaccinated patients. HD and patient DCs expressed the co-inhibitory molecules PD-1, LAG-3, PD-L1, PD-L2, and CTLA-4 at baseline (iDCs), then lost surface expression of PD-1 and LAG-3 post-maturation. In contrast, HD and melanoma patient DCs expressed higher PD-L1, PD-L2, and CTLA-4 post-maturation and after adenoviral transduction (Supplementary Fig. S4A). We observed a significant direct correlation between CTLA-4 and PD-L1 surface expression on patient AdVTMM2/DC (Supplementary Fig. S4B). Transcriptional profiling of patient DCs was also performed, revealing significant changes in gene expression due to maturation, with additional changes post-AdVTMM2 antigen engineering. *CTLA4* mRNA expression in AdVTMM2/DC was inversely correlated to mRNA transcript levels of the costimulatory molecule, *CD80*, and the Th1-polarizing cytokine subunit, *IL12p35* (Supplementary Fig. S4C). We also determined that *CTLA4* mRNA expression in AdVTMM2/DC was positively associated with *IL10* mRNA expression (Supplementary Fig. S4C). Transcriptional profiling and protein analyses of patient DCs revealed that melanoma patients had high expression of immunoregulatory molecules, including *IL10* and *IDO* (Supplementary Fig. S2C–D). Although it is known that the maturation of DCs leads to increased stimulatory capacity, these data suggest a compensatory turn-on of regulatory networks that could contribute to limitations in the ability of DCs to activate T cells.

ICOSL cell surface protein expression is reduced on patient DCs

The protein screen revealed that both HD and melanoma patient DCs rarely expressed B7-H4 and B7-H5. Surface expression of the costimulatory molecule ICOSL was reduced on both patient and HD DCs upon maturation and subsequent viral transduction (Fig. 1A, Supplementary Fig. S1). The expression of ICOSL on patient-derived DCs was significantly lower than that of DCs from HDs (Fig. 1A, Supplementary Fig. S1), and patients exhibited a more significant decrease in ICOSL cell surface expression when iDCs were matured (Supplementary Fig. S5A). Clinical outcomes were not correlated with ICOSL surface protein expression, although significant negative correlations were identified between surface ICOSL expression and IL10 production from patient mDCs and AdVTMM2/DC (Fig. 1B). Unlike the maturation-induced changes observed with co-inhibitory molecules, ICOSL was the only molecule observed to have a patient-specific impact association.

ICOSLG iDC mRNA expression correlates with clinical outcome and OS in melanoma patients

Transcriptional profiling of patient iDCs, mDCs, and AdVTMM2/DC revealed no significant differences in *ICOSLG* mRNA expression. However, it was observed that

baseline expression of *ICOSLG* correlated with favorable clinical outcome (Fig. 1C, middle). Survival analysis revealed that higher *ICOSLG* expression at baseline was associated with longer OS and PFS in patients (Fig. 1D). No direct association was observed with mDC or AdVTMM2/DC *ICOSLG* expression and survival. When patients were separated by clinical outcome, *IL12B (IL12p40)* expression had a significant positive association with *ICOSLG* expression (Fig. 1E) in AdVTMM2/DC. Analysis of publicly available datasets identified significant positive associations among *ICOSLG* expression, CD8^{+} T-cell infiltration at sites of metastasis in skin cutaneous melanomas, and favorable clinical outcomes, further supporting the potential importance of ICOSL in activating protective T-cell responses (Supplementary Fig. S5C–D).

sICOSL concentrations from patient mDCs positively associate with overall survival rates

The transcriptional analysis of patient DCs indicated that baseline expression of *ICOSLG* increased post-maturation (Fig. 1C, right and left panels), which was not reflected by the ICOSL surface protein expression. Therefore, post-translational processing in DCs, such as shedding, was investigated. sICOSL concentrations were detected in patient and HD DC culture supernatants. sICOSL increased significantly post-maturation in patient cells (Fig. 2A), which might explain the differences observed between mRNA expression and protein expression of ICOSL. sICOSL concentrations from patient mDCs correlated with clinical outcome (Fig. 2A). No significant changes were observed in sICOSL from HD DCs post-maturation (Fig. 2B). Survival analysis comparing sICOSL from patient mDCs revealed that higher production of sICOSL was associated with longer OS and PFS rates (Fig. 2C). sICOSL secretion from patient mDCs significantly correlated with Th1-polarizing chemokines, MIP-1α and CXCL9 (Fig. 2D). sICOSL was also detected 24hrs. post-viral transduction in AdVTMM2/DC supernatants from both HDs and patients (Supplementary Fig. S5B).

ICOSL expression on patient DCs is associated with *in vivo* T-cell responses

We hypothesized that DC ICOSL expression may be important for the generation of optimal immune responses. ICOSL surface protein expression on patient AdVTMM2/DC was positively associated (p=0.002) with the ability of these antigen-presenting cells to induce specific CD8^{+} T-cell responses against tyrosinase *in vivo* (Fig. 3A). Increased sICOSL positively correlated with the magnitude of aggregate vaccine-induced CD8^{+} T-cell responses (Fig. 3B), suggesting the functional importance of sICOSL in antitumor immunity. Calculated hazard ratios indicated that sICOSL was a positive predictive prognostic factor for OS and PFS in these patients, whereas surface ICOSL on AdVTMM2/DC was a positive predictive index only for OS (Table 1). Together, these data suggest that ICOSL might be important for antigen-specific T-cell responses.

DC-expressed ICOSL is critical for the priming of antigen-specific T-cell responses

To determine if the expression of ICOSL on DCs was critical for the initiation of T-cell activation or for recall responses *in vitro*, we chose a model of priming or boosting T cells using cytomegalovirus (CMV) pp65 antigen. HDs were identified as CMV-naïve or CMV-experienced based on serum antibody (IgG, IgM) reactivity against CMV. Autologous mDCs were cultured with or without blocking ICOSL and pulsed with a CMV pp65 peptide pool.

CD4^{+} and CD8^{+} T cells primed with ICOSL-blocked DCs expressed less CD107a and produced significantly less granzyme-B than T cells primed using ICOSL-expressing DCs (Fig. 3C). In contrast, we observed no impact for ICOSL blockade on recall T-cell responses to CMV (Fig 3D). These data suggests that ICOSL expression on DCs plays a role in optimal (cross)priming of effector CD8^{+} and CD4^{+} T cells and does not play a dominant role in modulating recall responses.

NF-κB signaling is dysregulated in patient DCs

To investigate molecular pathways responsible for the deficiency in surface expression of ICOSL on patient DCs, gene expression profiles from patient iDCs, mDCs, and vaccines were analyzed. Differentially expressed genes in iDCs and mDCs from patients were compared to HD DCs.

Patient mDCs exhibited profiles with dysregulated metabolic, toll-like receptor, IL8, and NF-κB signaling pathways (Fig. 4A). Of these, the predicted dysregulation of the NF-κB pathway was of interest because the noncanonical NF-κB signaling pathway has been previously reported to regulate *ICOSLG* expression in murine B cells (21). Microarray data revealed significant increases in expression of *NFKBID*, an inhibitor of the NF-κB signaling pathway, in patient mDCs. No changes in *NFKBID* mRNA expression was observed in HD mDCs (Fig. 4B). To further investigate the NF-κB dysregulation observed in patients, inflammatory and Th1-polarizing molecules known to be regulated by NF-κB pathway were examined in post-maturation supernatants from patient and HD DCs. Expression of cytokines and chemokines revealed that patient mDCs had lower expression of soluble TNFα, soluble CD40L, and CXCL9 compared to HD mDCs (Fig. 4C). The secretion of these important molecules, including CXCL11, were enhanced in patients with favorable clinical outcomes (Fig. 4C). Functional validation of the aberrant canonical NF-κB signaling in patient DCs was confirmed using cellular imaging. HD DCs showed an expected significant increase in NF-κB p65 translocation from cytoplasm into the nucleus upon *ex vivo* maturation, which was not observed for patient DCs (Fig. 4D–E).

NF-κB p65 is a Direct Transcriptional Regulator of *ICOSLG*

After observing operational NF-κB dysregulation in patient matured DCs, we hypothesized that *ICOSLG* expression might be dependent on canonical NF-κB signaling. To investigate this, we analyzed direct binding of NF-κB p65 to the *ICOSLG* promoter region. Chromatin immunoprecipitation revealed a direct p65 binding to the *ICOSLG* gene promoter in HD mDCs (Fig. 5A, Supplementary Fig. S6). To further confirm the role of NF-κB on ICOSL regulation, we assessed the impact of adding the NF-κB inhibitor, parthenolide [which directly modifies the p65 subunit by inhibiting IkB proteins (22,23)], on surface ICOSL after DC maturation. The inhibition of NF-κB activation resulted in a significant decrease in phospho-p65 in the parthenolide-treated DC group (Fig. 5B–C). ICOSL surface protein levels were significantly decreased in Parthenolide-treated DC compared to control DC (Fig. 5B–C), showing that canonical NF-κB signaling regulated ICOSL surface protein expression in DCs.

Inhibition of ADAM10/17 sheddase activity stabilizes ICOSL surface expression

We have shown that canonical NF-κB signaling regulated ICOSL surface protein expression. However, our data also suggested that ICOSL was shed from the DC surface, which correlated with clinical outcome. Our microarray data revealed that patient DCs expressed the metalloproteases ADAM10 and ADAM17. ADAM10 was significantly reduced post-maturation, whereas ADAM17 expression increased (Fig. 6A). To investigate the mechanisms underlying the shedding of surface ICOSL, we inhibited ADAM10/17 activity, using Tapi-2, during DC maturation (14,15). HD DCs matured in the presence of Tapi-2 exhibited a significant increase in surface ICOSL and decrease in sICOSL (Fig. 6B–C). These data suggest that both canonical NF-κB signaling and metalloproteinase activity contributed to the regulation of ICOSL in DCs.

Discussion

In this study, we have shown that expression of many of the key antigen presentation (MHC class I and II) and costimulatory molecules (CD40, CD80, CD86) focused on in previous human DC vaccines trials as biomarkers of potency in patients did not correlate with immune or clinical response to an autologous AdVTMM2/DC-based vaccine in 35 advanced-stage melanoma patients (12). We were unable to validate IL12p70 secretion as a biomarker for time to progression, as suggested in some previous DC-based vaccine trials (19,20). These data suggest the operational relevance of alternate molecules and pathways in the efficacy of DC vaccines in patients with advanced-stage melanoma.

Based on the observation that classical DC markers did not correlate with clinical responsiveness, we sought to identify molecules and signaling pathways that impacted DC-induced patient T-cell responses and clinical outcomes. We initially investigated eleven costimulatory and co-inhibitory molecules known to impact DC antigen presentation and T-cell activation. Protein expression of these checkpoint and costimulatory molecules was directly examined in iDCs, mDCs, and AdVTMM2/DC. PD-L1, PD-L2, and CTLA-4 were significantly upregulated post-maturation. PD-L1 and CTLA-4 have both been independently shown to be regulated by JAK2 and STAT1 through IFNγ signaling, which may explain the increase in surface expression of these molecules (24,25). We have previously shown that the blockade of PD-1 during recall antigen presentation by DCs had minimal impact on induced T-cell responses (26). However, here, *CTLA4* mRNA expression correlated negatively with *CD86*, *CD80* and *IL12p35* mRNA expression in patient DCs and was positively correlated with *IL10* mRNA. Together, these findings suggested that melanoma patient-derived DCs were hypo-stimulatory and suggest areas for targeted improvement.

We identified ICOSL as being differentially expressed between patient and HD DCs. Differential surface protein expression of ICOSL was observed between HDs and patients. iDCs, mDCs, and AdVTMM2/DC from patients displayed lower surface expression of ICOSL compared to HDs. There was a gradual decline in ICOSL expression post-maturation in both HDs and patients, which differs from what has been previously reported for monocyte-derived DCs from healthy donors (27). We have shown that surface ICOSL expression on AdVTMM2/DC was negatively associated with IL10. ICOSL surface

expression on AdVTMM2/DC also significantly correlated with vaccine-induced tyrosinase-specific CD8^{+} T-cell responses. Increased *ICOSLG* expression in DC vaccines had a significant positive correlation with *IL12B* expression. This suggests that surface expression of ICOSL DC may be critical for the activation of T-cell responses in melanoma patients.

ICOSL has also been previously reported to be shed from B cells based on the action of the sheddase ADAM10 (28). By cleaving surface ICOSL, ADAM10 modulates availability of ICOSL costimulation during humoral immune activation (28). Our microarray data revealed that patient DCs expressed ADAM10 and significantly increased mRNA transcript levels of another metalloproteinase molecule, ADAM17, post-maturation. Here, we have shown that inhibition of ADAM10/17 sheddase activity, in addition to the possible inhibition of other metalloproteases, in DCs increased surface expression of ICOSL and decreased sICOSL, revealing the importance of metalloproteinase activity in regulating ICOSL surface expression. To our knowledge, the importance of ADAM10/17 sheddase activity for ICOSL regulation on human DCs has not yet been reported. We have also shown that sICOSL increased in mDC cultures from patients with favorable outcomes and correlates with survival rates, suggesting that sICOSL may represent a biomarker for clinical responsiveness.

Although it has been previously reported that ICOSL expression on activated antigen-presenting cells plays a critical costimulatory role for T-cell activation (27), the physiological role for soluble ICOSL is not well understood. Plasma sICOSL is significantly increased in patients with acute pancreatitis, and its elevated expression is associated with disease severity in patients with systemic lupus erythematous (29,30). Here, we showed significant positive correlations between sICOSL and antigen-specific CD8^{+} T-cell responses and survival rates in melanoma patients. We also observed higher sICOSL production from patient mDCs, which was significantly correlated with the Th1 chemokines, MIP-1α and CXCL9. We further showed continuous production of sICOSL by HD and patient AdVTMM2/DC. When taken together, these data point to the importance of cell surface, as well as shed ICOSL, as biomarkers for the clinical efficacy of autologous DC vaccination in melanoma patients. Prospective studies exploring the physiological role of sICOSL in regulating antitumor T-cell responses will be of significant interest.

ICOS signaling has been reported to mediate both immunoregulatory and immunostimulatory roles in the cancer setting. Some studies show that increased expression of ICOSL on tumor cells is associated with disease progression and poor clinical outcome (31), and high expression of ICOSL on cancer cells facilitates development of immunosuppressive CD4^{+} T cells (32). Conversely, studies in colon cancer show that high ICOS expression on infiltrating leukocytes is associated with better overall survival (33). In patients previously treated with anti-CTLA-4, high ICOS expression on T cells is associated with better prognosis (34). Treatment with vaccines engineered to express ICOSL, along with co-administered CTLA-4 blockade, increases T-cell responses in prostate and melanoma mouse models, suggesting an important role of ICOS signaling in the development of antitumor immunity (35).

The positive linear associations observed between ICOSL and patient CD8^{+} antigen-specific T-cell responses, as well as survival rates, implicated ICOSL as having potential functional importance in DC-mediated (cross)priming of antigen-specific T-cell responses *in vivo*. This was not addressed in the late-stage cancer patients, whose PBMCs were primarily memory T cells or exhausted effector T cells (12). To properly investigate this paradigm, we employed a CMV-based *in vitro* vaccine model, assessing T-cell expression of granzyme-B and CD107a as effector cell cytotoxic activity (36). We showed that CD8^{+} T cells from CMV-seronegative donors primed with antigen-loaded DCs (pretreated with anti-ICOSL) were significantly impaired in their ability to differentiate into effector T cells. DCs had high surface expression of the costimulatory molecule CD86, stressing a key differential early role for DC-expressed ICOSL in initiating responses from antigen-naïve T cells.

In the context of melanoma, CD4^{+} cytotoxic T cells have been isolated from patients in high frequencies, and these cells can kill autologous MHCII^{high} melanoma tumor cells. Murine models have indicated antigen-specific CD4^{+} T cells can aid in the expansion of infiltrating CD8^{+} T cells (37). Murine and human studies have both shown that anti-PD1 and anti-CTLA-4 treatment increases the cytotoxic activity of these cells, indicting an important role for CD4^{+} T cells in anti-tumor immunity (38,39). In the CMV-based *in vitro* vaccine model, we showed that CD4^{+} T cells primed with pretreated anti-ICOSL antigen-loaded DCs were functionally impaired. These data revealed that ICOSL was critical for the priming of cytotoxic antigen-specific CD4^{+} and CD8^{+} T cells, and both CD4^{+} and CD8^{+} T cells impact antitumor immunity in melanoma patients. This suggests that increasing expression of ICOSL on patient DCs may improve antigen-specific vaccine responses in cancer patients.

Our data further revealed that ICOSL is in part by canonical NF-κB signaling, with p65 directly interacting with the promoter region of *ICOSLG*. To our knowledge, this regulation in DCs has not been previously reported, as only the noncanonical pathway of NF-κB signaling has been suggested to regulate ICOSL expression (21). We also showed that mDCs generated from patients exhibited a decrease in canonical NF-κB signaling, as evidenced by significant reductions in nuclear translocation of p65 compared to HD counterparts.

As predicted by dysregulation of NF-κB signaling, proinflammatory cytokine secretion was also reduced in cell culture supernatants from patient DCs. CXCL9, TNFα, soluble CD40L, and CXCL11 secretion from mDCs correlated with clinical outcome. CXCL11 secretion from mDCs seemed to be unique to melanoma patients, as CXCL11 production from HD mDCs was marginal. The observed correlation with clinical efficiency indicated these molecules may represent salient biomarkers for assessing clinical efficiency in patients. The decreased activation of the canonical NF-κB signaling pathway did not affect the maturation-induced upregulation of the costimulatory molecule CD86. This finding can be explained by CD86 regulation in human DCs by RelB, which is predominately associated with noncanonical NF-κB signaling pathway (40). Complementary pathways are being investigated, such as IFNγ signaling, which is reported to upregulate CD86 expression (41).

The comparative pathway analysis revealed that matured DCs from melanoma patients have increased transcriptional expression of natural NF-κB inhibitors post-maturation. Some of these inhibitors, such as NFκBIA, are regulatory molecules that are transcriptionally

activated upon NF-κB activation. Transcripts of these molecules were increased in both patient and healthy donor cells. However, transcriptional expression of the inhibitor molecule, *NFκBID*, was only upregulated in patient DCs post-maturation. This was of interest because previous studies show that *NFκBID* expression in DCs leads to an immunoregulatory phenotype with increased secretion of IL10 (42). Transcriptional profiling and protein analyses of patient DCs showed that melanoma patients had high expression of immunoregulatory molecules, such as IL10 and *IDO*. Overall, these data indicated that genetic manipulation of NF-κB targets in patient DCs may mitigate their immunoregulatory phenotype and lead to increased expression of costimulatory and proinflammatory molecules believed critical to the efficacy of DC-based vaccines. This dysregulation of canonical NF-κB signaling in patients may in part explain the observed reductions in ICOSL protein expressed on the surface of DCs cultured from melanoma patients. Indeed, we showed that NF-κB signaling, via both the canonical and noncanonical pathways, was important for DC immunogenicity and the anti-tumor efficacy of DC-based vaccines (40,43–45).

In summary, this study revealed that canonical NF-κB signaling and ADAM10/17 sheddase activity were critical for the regulation of ICOSL gene and protein expression in DCs. Our data suggest that the dysregulation in NF-κB signaling and the expression of ADAM10/17 may explain the decrease in ICOSL protein surface expression observed in patient DCs. We identified ICOSL as a potential potency biomarker for the *in vivo* immunogenicity of DC-based vaccines in melanoma patients. Reduced expression of ICOSL on monocyte-derived DC limited their ability to prime antitumor immune responses *in vitro* and *in vivo*. We also showed that baseline mRNA expression of *ICOSLG* on patient DCs correlated with favorable clinical outcomes and associated with overall patient survival, suggesting the clinical associations observed with ICOSL may be imprinted in dysregulated patient precursor cells. Future studies will involve the profiling of HD and patient monocytes and investigate epigenetic changes within these cells that may underlie dysregulated ICOSL expression. It will also be important to determine the impact of enforced DC expression of ICOSL on vaccine-induced, antigen-specific T-cell responses in patients. Conditioning of increased ICOSL on patient DCs may yield a vaccine capable of more effectively driving the development of clinically effective antitumor immunity in support of superior clinical outcomes.

Supplementary Material

Refer to Web version on PubMed Central for supplementary material.

Acknowledgements

References Cited

1. Siegel RL, Miller KD, Jemal A. Cancer statistics, 2019. CA Cancer J Clin 2019;69(1):7–34 doi 10.3322/caac.21551. [PubMed: 30620402]

2. Hodi FS, O'Day SJ, McDermott DF, Weber RW, Sosman JA, Haanen JB, et al. Improved survival with ipilimumab in patients with metastatic melanoma. N Engl J Med 2010;363(8):711–23 doi 10.1056/NEJMoa1003466. [PubMed: 20525992]

3. Ribas A, Wolchok JD, Robert C, Kefford R, Hamid O, Daud A, et al. Updated clinical efficacy of the anti-PD-1 monoclonal antibody pembrolizumab (MK-3475) in 411 patients with melanoma. European Journal of Cancer 2015;51(24) doi 10.1016/j.ejca.2015.06.072.

4. Yuan J, Ginsberg B, Page D, Li Y, Rasalan T, Gallardo HF, et al. CTLA-4 blockade increases antigen-specific CD8(+) T cells in prevaccinated patients with melanoma: three cases. Cancer Immunol Immunother 2011;60(8):1137–46 doi 10.1007/s00262-011-1011-9. [PubMed: 21465316]

5. Wolchok JD, Kluger H, Callahan MK, Postow MA, Rizvi NA, Lesokhin AM, et al. Nivolumab plus ipilimumab in advanced melanoma. N Engl J Med 2013;369(2):122–33 doi 10.1056/NEJMoa1302369. [PubMed: 23724867]

6. Curtsinger JM, Schmidt CS, Mondino A, Lins DC, Kedl RM, Jenkins MK, et al. Inflammatory cytokines provide a third signal for activation of naive CD4+ and CD8+ T cells. J Immunol 1999;162(6):3256–62. [PubMed: 10092777]

7. Lafferty KJ, Warren HS, Woolnough JA. A mediator acting as a costimulator for the development of cytotoxic responses in vitro. Adv Exp Med Biol 1979;114:497–501 doi 10.1007/978-1-4615-9101-6_82. [PubMed: 313677]

8. Zinkernagel RM, Doherty PC. Restriction of in vitro T cell-mediated cytotoxicity in lymphocytic choriomeningitis within a syngeneic or semiallogeneic system. Nature 1974;248(5450):701–2 doi 10.1038/248701a0. [PubMed: 4133807]

9. Santos PM, Butterfield LH. Dendritic Cell-Based Cancer Vaccines. J Immunol 2018;200(2):443–9 doi 10.4049/jimmunol.1701024. [PubMed: 29311386]

10. Nestle FO, Alijagic S, Gilliet M, Sun Y, Grabbe S, Dummer R, et al. Vaccination of melanoma patients with peptide- or tumor lysate-pulsed dendritic cells. Nat Med 1998;4(3):328–32 doi 10.1038/nm0398-328. [PubMed: 9500607]

11. Rosenberg SA, Yang JC, Restifo NP. Cancer immunotherapy: moving beyond current vaccines. Nat Med 2004;10(9):909–15 doi 10.1038/nm1100. [PubMed: 15340416]

12. Butterfield LH, Vujanovic L, Santos PM, Maurer DM, Gambotto A, Lohr J, et al. Multiple antigen-engineered DC vaccines with or without IFNalpha to promote antitumor immunity in melanoma. J Immunother Cancer 2019;7(1):113 doi 10.1186/s40425-019-0552-x. [PubMed: 31014399]

13. Blalock LT, Landsberg J, Messmer M, Shi J, Pardee AD, Haskell R, et al. Human dendritic cells adenovirally-engineered to express three defined tumor antigens promote broad adaptive and innate immunity. Oncoimmunology 2012;1(3):287–357 doi 10.4161/onci.18628. [PubMed: 22737604]

14. Wang R, Ye X, Bhattacharya R, Boulbes DR, Fan F, Xia L, et al. A Disintegrin and Metalloproteinase Domain 17 Regulates Colorectal Cancer Stem Cells and Chemosensitivity Via Notch1 Signaling. Stem Cells Transl Med 2016;5(3):331–8 doi 10.5966/sctm.2015-0168. [PubMed: 26744411]

15. Moss ML, Rasmussen FH. Fluorescent substrates for the proteinases ADAM17, ADAM10, ADAM8, and ADAM12 useful for high-throughput inhibitor screening. Anal Biochem 2007;366(2):144–8 doi 10.1016/j.ab.2007.04.043. [PubMed: 17548045]

16. Jin P, Han TH, Ren J, Saunders S, Wang E, Marincola FM, et al. Molecular signatures of maturing dendritic cells: implications for testing the quality of dendritic cell therapies. J Transl Med 2010;8:4 doi 10.1186/1479-5876-8-4. [PubMed: 20078880]

17. Carvalho BS, Irizarry RA. A framework for oligonucleotide microarray preprocessing. Bioinformatics 2010;26(19):2363–7 doi 10.1093/bioinformatics/btq431. [PubMed: 20688976]

18. Ritchie ME, Phipson B, Wu D, Hu Y, Law CW, Shi W, et al. limma powers differential expression analyses for RNA-sequencing and microarray studies. Nucleic Acids Res 2015;43(7):e47 doi 10.1093/nar/gkv007. [PubMed: 25605792]

19. Carreno BM, Becker-Hapak M, Huang A, Chan M, Alyasiry A, Lie WR, et al. IL-12p70-producing patient DC vaccine elicits Tc1-polarized immunity. J Clin Invest 2013;123(8):3383–94 doi 10.1172/JCI68395. [PubMed: 23867552]

20. Okada H, Kalinski P, Ueda R, Hoji A, Kohanbash G, Donegan TE, et al. Induction of CD8+ T-cell responses against novel glioma-associated antigen peptides and clinical activity by vaccinations with {alpha}-type 1 polarized dendritic cells and polyinosinic-polycytidylic acid stabilized by lysine and carboxymethylcellulose in patients with recurrent malignant glioma. J Clin Oncol 2011;29(3):330–6 doi 10.1200/JCO.2010.30.7744. [PubMed: 21149657]

21. Hu H, Wu X, Jin W, Chang M, Cheng X, Sun SC. Noncanonical NF-kappaB regulates inducible costimulator (ICOS) ligand expression and T follicular helper cell development. Proc Natl Acad Sci U S A 2011;108(31):12827–32 doi 10.1073/pnas.1105774108. [PubMed: 21768353]

22. Kwok BH, Koh B, Ndubuisi MI, Elofsson M, Crews CM. The anti-inflammatory natural product parthenolide from the medicinal herb Feverfew directly binds to and inhibits IkappaB kinase. Chem Biol 2001;8(8):759–66 doi 10.1016/s1074-5521(01)00049-7. [PubMed: 11514225]

23. Saadane A, Masters S, DiDonato J, Li J, Berger M. Parthenolide inhibits IkappaB kinase, NF-kappaB activation, and inflammatory response in cystic fibrosis cells and mice. Am J Respir Cell Mol Biol 2007;36(6):728–36 doi 10.1165/rcmb.2006-0323OC. [PubMed: 17272824]

24. Garcia-Diaz A, Shin DS, Moreno BH, Saco J, Escuin-Ordinas H, Rodriguez GA, et al. Interferon Receptor Signaling Pathways Regulating PD-L1 and PD-L2 Expression. Cell Rep 2017;19(6):1189–201 doi 10.1016/j.celrep.2017.04.031. [PubMed: 28494868]

25. Mo X, Zhang H, Preston S, Martin K, Zhou B, Vadalia N, et al. Interferon-gamma Signaling in Melanocytes and Melanoma Cells Regulates Expression of CTLA-4. Cancer Res 2018;78(2):436–50 doi 10.1158/0008-5472.CAN-17-1615. [PubMed: 29150430]

26. Santos PM, Adamik J, Howes TR, Du S, Vujanovic L, Warren S, et al. Impact of checkpoint blockade on cancer vaccine-activated CD8+ T cell responses. J Exp Med 2020;217(7) doi 10.1084/jem.20191369.

27. Aicher A, Hayden-Ledbetter M, Brady WA, Pezzutto A, Richter G, Magaletti D, et al. Characterization of human inducible costimulator ligand expression and function. J Immunol 2000;164(9):4689–96 doi 10.4049/jimmunol.164.9.4689. [PubMed: 10779774]

28. Lownik JC, Luker AJ, Damle SR, Cooley LF, El Sayed R, Hutloff A, et al. ADAM10-Mediated ICOS Ligand Shedding on B Cells Is Necessary for Proper T Cell ICOS Regulation and T Follicular Helper Responses. J Immunol 2017;199(7):2305–15 doi 10.4049/jimmunol.1700833. [PubMed: 28814605]

29. Her M, Kim D, Oh M, Jeong H, Choi I. Increased expression of soluble inducible costimulator ligand (ICOSL) in patients with systemic lupus erythematosus. Lupus 2009;18(6):501–7 doi 10.1177/0961203308099176. [PubMed: 19395451]

30. Huang J, Wu Z, Lu S, Shen J, Kong X, Shen Y. Soluble B7-H2 as a novel marker in early evaluation of the severity of acute pancreatitis. Lab Med 2015;46(2):109–17 doi 10.1309/LMFSRH0V82HFXPPI. [PubMed: 25918189]

31. Wang B, Jiang H, Zhou T, Ma N, Liu W, Wang Y, et al. Expression of ICOSL is associated with decreased survival in invasive breast cancer. PeerJ 2019;7:e6903 doi 10.7717/peerj.6903. [PubMed: 31143539]

32. Faget J, Sisirak V, Blay JY, Caux C, Bendriss-Vermare N, Menetrier-Caux C. ICOS is associated with poor prognosis in breast cancer as it promotes the amplification of immunosuppressive CD4(+) T cells by plasmacytoid dendritic cells. Oncoimmunology 2013;2(3):e23185 doi 10.4161/onci.23185. [PubMed: 23802069]

33. Zhang Y, Luo Y, Qin SL, Mu YF, Qi Y, Yu MH, et al. The clinical impact of ICOS signal in colorectal cancer patients. Oncoimmunology 2016;5(5):e1141857 doi 10.1080/2162402X.2016.1141857. [PubMed: 27467961]

34. Carthon BC, Wolchok JD, Yuan J, Kamat A, Ng Tang DS, Sun J, et al. Preoperative CTLA-4 blockade: tolerability and immune monitoring in the setting of a presurgical clinical trial. Clin Cancer Res 2010;16(10):2861–71 doi 10.1158/1078-0432.CCR-10-0569. [PubMed: 20460488]

35. Fan X, Quezada SA, Sepulveda MA, Sharma P, Allison JP. Engagement of the ICOS pathway markedly enhances efficacy of CTLA-4 blockade in cancer immunotherapy. J Exp Med 2014;211(4):715–25 doi 10.1084/jem.20130590. [PubMed: 24687957]

36. Betts MR, Brenchley JM, Price DA, De Rosa SC, Douek DC, Roederer M, et al. Sensitive and viable identification of antigen-specific CD8+ T cells by a flow cytometric assay for degranulation. J Immunol Methods 2003;281(1–2):65–78 doi 10.1016/s0022-1759(03)00265-5. [PubMed: 14580882]

37. Wong SB, Bos R, Sherman LA. Tumor-specific CD4+ T cells render the tumor environment permissive for infiltration by low-avidity CD8+ T cells. J Immunol 2008;180(5):3122–31 doi 10.4049/jimmunol.180.5.3122. [PubMed: 18292535]

38. Quezada SA, Simpson TR, Peggs KS, Merghoub T, Vider J, Fan X, et al. Tumor-reactive CD4(+) T cells develop cytotoxic activity and eradicate large established melanoma after transfer into lymphopenic hosts. J Exp Med 2010;207(3):637–50 doi 10.1084/jem.20091918. [PubMed: 20156971]

39. Yan H, Hou X, Li T, Zhao L, Yuan X, Fu H, et al. CD4+ T cell-mediated cytotoxicity eliminates primary tumor cells in metastatic melanoma through high MHC class II expression and can be enhanced by inhibitory receptor blockade. Tumour Biol 2016 doi 10.1007/s13277-016-5456-5.

40. Shih VF, Davis-Turak J, Macal M, Huang JQ, Ponomarenko J, Kearns JD, et al. Control of RelB during dendritic cell activation integrates canonical and noncanonical NF-kappaB pathways. Nat Immunol 2012;13(12):1162–70 doi 10.1038/ni.2446. [PubMed: 23086447]

41. Mir MA. Developing costimulatory molecules for immunotherapy of diseases. Chapter 1 - Introduction to Costimulation and Costimulatory Molecules. Amsterdam: Elsevier/Academic Press,; 2015. p 1–43.

42. Fujita S, Seino K, Sato K, Sato Y, Eizumi K, Yamashita N, et al. Regulatory dendritic cells act as regulators of acute lethal systemic inflammatory response. Blood 2006;107(9):3656–64 doi 10.1182/blood-2005-10-4190. [PubMed: 16410444]

43. Ouaaz F, Arron J, Zheng Y, Choi Y, Beg AA. Dendritic cell development and survival require distinct NF-kappaB subunits. Immunity 2002;16(2):257–70 doi 10.1016/s1074-7613(02)00272-8. [PubMed: 11869686]

44. Wang J, Wang X, Hussain S, Zheng Y, Sanjabi S, Ouaaz F, et al. Distinct roles of different NF-kappa B subunits in regulating inflammatory and T cell stimulatory gene expression in dendritic cells. J Immunol 2007;178(11):6777–88 doi 10.4049/jimmunol.178.11.6777. [PubMed: 17513725]

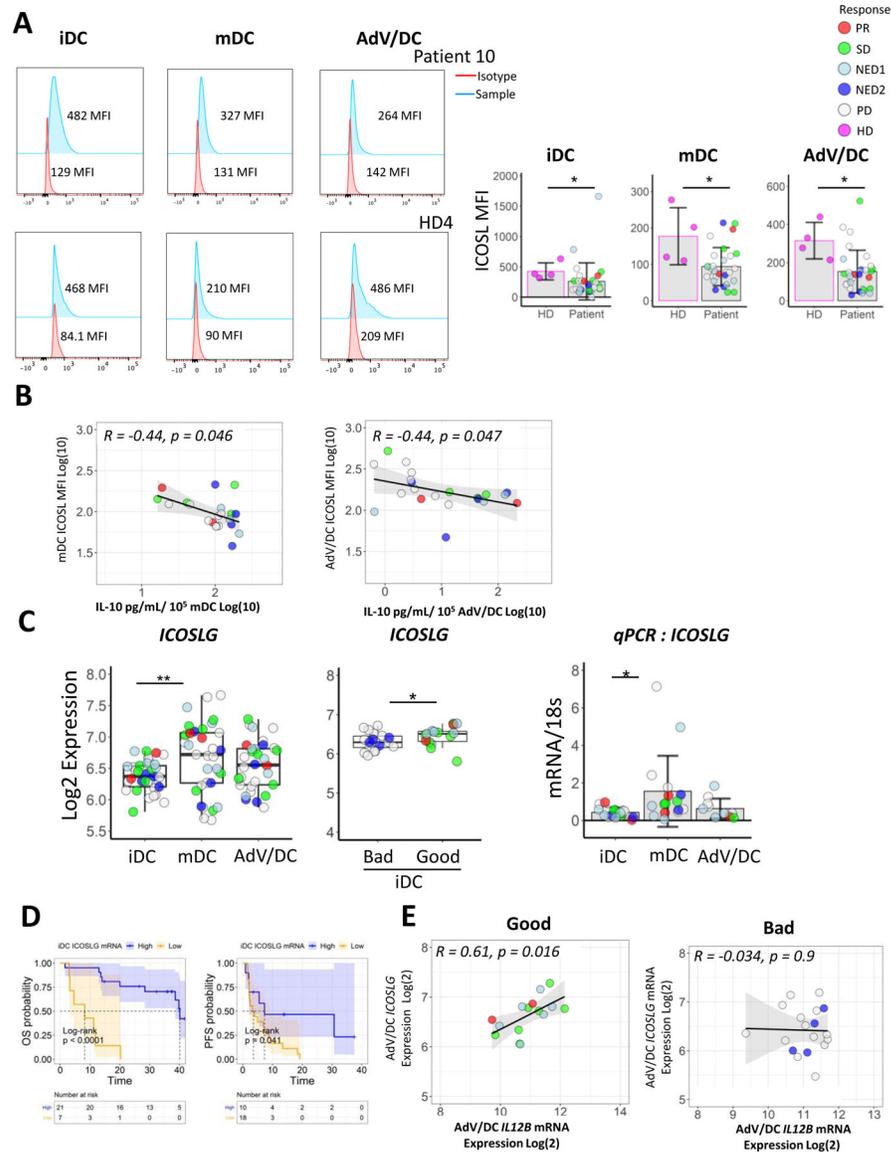45. Kawai T, Akira S. TLR signaling. Semin Immunol 2007;19(1):24–32 doi 10.1016/j.smim.2006.12.004. [PubMed: 17275323]

Figure 1. ICOSL protein expression is reduced on melanoma patient DCs vs. healthy donor (HD) DCs and negatively correlates with IL10.

(A) ICOSL protein surface expression was analyzed on melanoma patient (n=30) DC subtypes and HDs (n=4) by flow cytometry. Representative histograms from a patient and HD are shown for each DC subtype. Background staining was corrected with isotype (red) controls (left). Quantified ICOSL MFI values are shown (right). Patients were segregated by clinical outcomes, with intergroup significance determined using unpaired Wilcoxon rank sum test. Error bars represent standard deviation. (B) Correlation of mDC and AdV/DC ICOSL and IL10 (n=22). The grey shaded area represents the 95% Confidence Interval bands. (C) Microarray and qPCR analysis of *ICOSLG* transcripts in patient DCs (n=33, iDC, mDC, AdV/DC). Patients were segregated by clinical outcomes, with intergroup significance determined using unpaired Kruskal-Wallis one-way ANOVA (left and right panels) or paired student t-test (one-tailed)(middle panel). Each end of the box and whisker plots represent the first (25%) and third (75%) quartile, while the middle line represents the

mean. (D) Kaplan-Meier (KM) curves showing OS and PFS in patients (n=33) based on iDC mRNA expression of *ICOSLG*. (E) Correlation of AdV/DC *ICOSLG* mRNA and *IL12B* mRNA expression in favorable clinical outcome patients (n=33). The grey shaded area represents the 95% Confidence Interval bands. Correlations were calculated using Pearson's correlation coefficients, and the data was log transformed to meet normality assumptions (E). *p 0.05, **p 0.01.
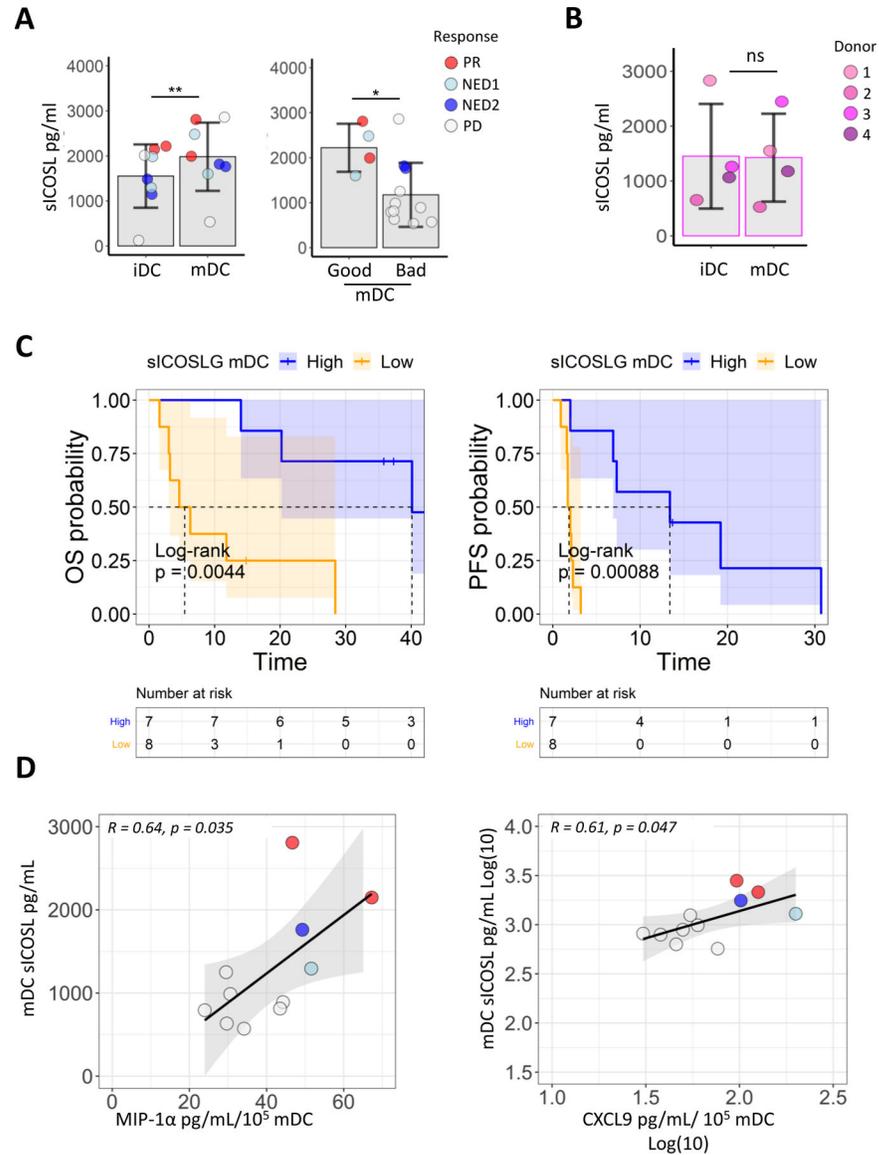
Figure 2. sICOSL correlates with favorable clinical outcomes, Th1 chemokines, and survival rates in patients.

(A-B) DC culture supernatants were tested using a specific ELISA. Error bars represent standard deviation. (A) Soluble ICOSL (sICOSL) was determined in patient (n=16) matched (n=8; iDC and mDC, left) and nonmatched (n=16, right) pairs. Patients were segregated by clinical outcomes, with intergroup significance determined using unpaired (left) or paired (right) Wilcoxon rank sum tests. (B) sICOSL of HD was determined in matched pairs (n=4). (C) KM curves showing OS and PFS in patients (n=15) based on mDC sICOSL. The log-rank p value is indicated. (D) Correlation of mDC sICOSL and Th1 chemokines, MIP-1α and CXCL9 (n=11). The grey shaded area represents the 95% Confidence Interval bands. Correlations were calculated using Pearson's correlation coefficients. The data was log transformed to meet normality assumptions (right panel). *p 0.05, **p 0.01, ns= not significant.

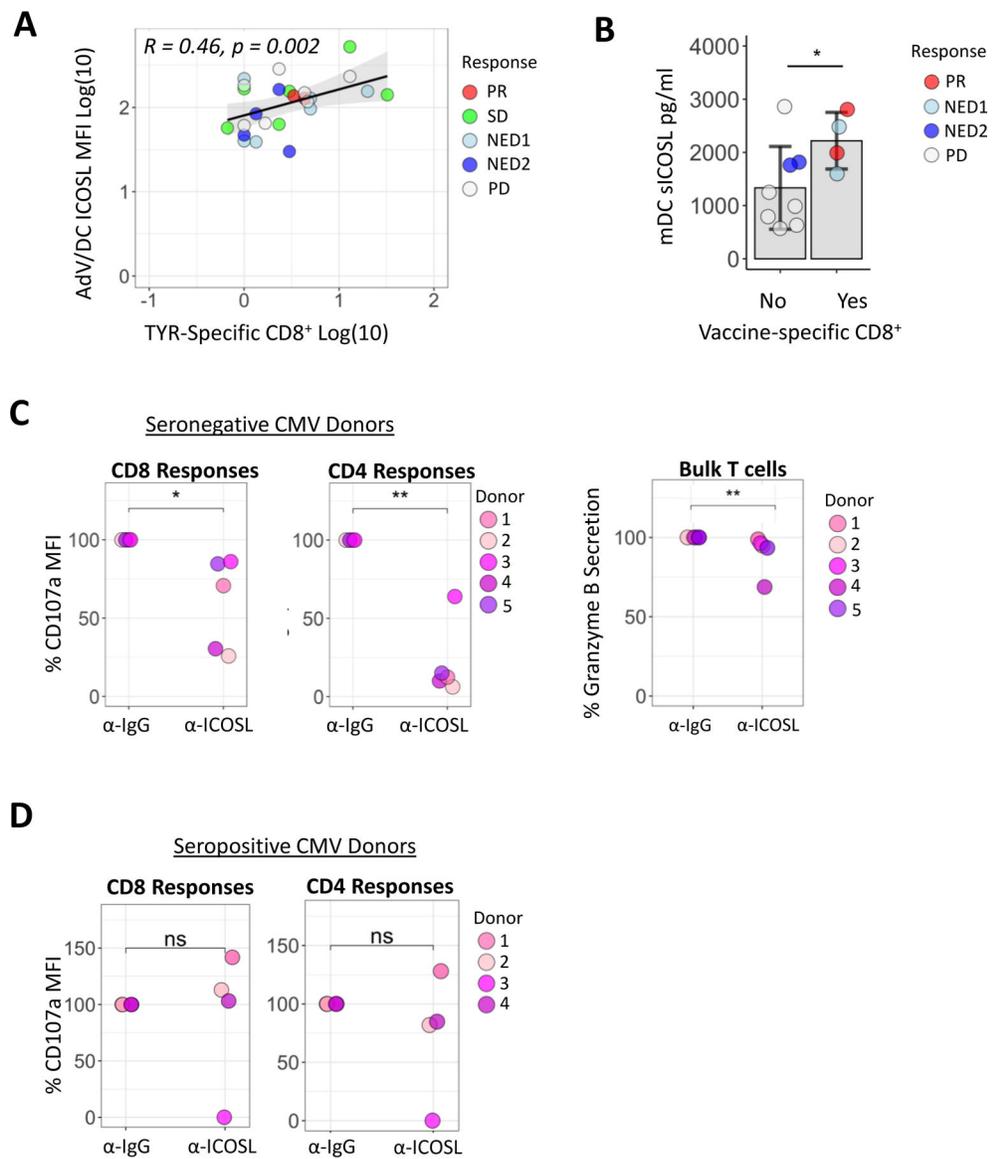**Figure 3. ICOSL on DC is critical for their ability to (cross)prime antigen-specific T-cell responses *in vitro*.**

(**A**) Correlation of ICOSL protein surface expression on AdV/DC and *in vivo* vaccine-specific tyrosinase CD8$^+$ T-cell responses (determined using IFNγ ELISPOT assays)(n=25; 12). The grey shaded area represents the 95% Confidence Interval bands. The data were log-transformed to meet normality assumptions. Pearson's R correlation was used to determine the correlation significance. (**B**) Soluble ICOSL detected in supernatants of patient mDCs based on bulk tumor-associated CD8$^+$ T-cell responses in patients (n=12). Error bars represent standard deviation. Patients were segregated by clinical outcomes, with intergroup significance determined using paired student t-tests. (**C-D**) CD107a MFI from CMV-specific T cells when (**C**) primed (n=5) or (**D**) boosted (n=4) with autologous mDCs previously treated with blocking anti-ICOSL (10 µg/mL) or IgG control. Granzyme-B secretion from CMV-specific T cells when primed with autologous mDCs previously treated with blocking anti-ICOSL or IgG control (n=5)(C). Data is displayed as normalized percentages against

the IgG control and unpaired Wilcoxon rank sum test was used to determine significance (C, D, E). *p 0.05, **p 0.01, ns= not significant.
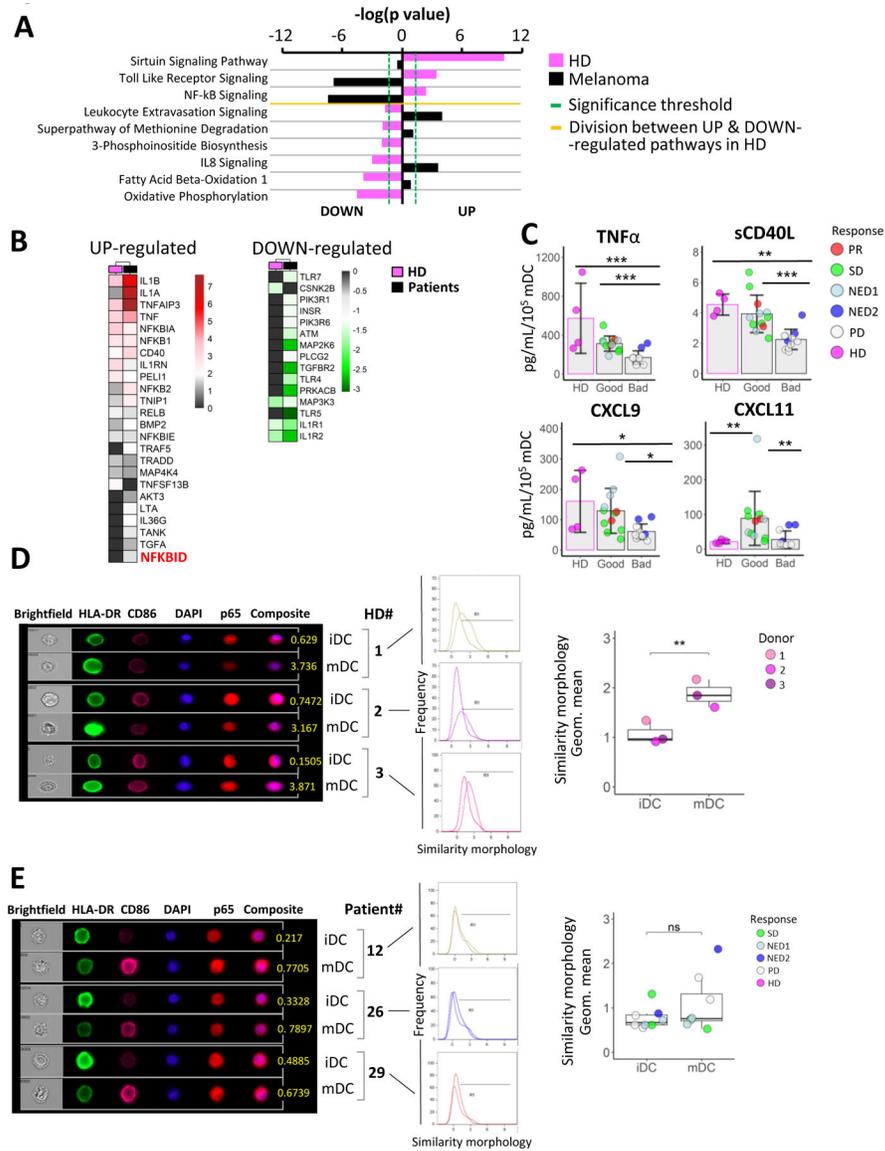
Figure 4. NF-κB signaling is dysregulated in melanoma patient vs. HD mDCs and expression of NF-κB targets correlate with clinical outcome.

(A) Comparative Ingenuity Pathway Analysis (IPA) of microarray data of mDCs from patients (n=35) compared to mDCs from HDs (n=6). The -log p values were calculated for each pathway, with a -log(0.05) considered to be significant (dashed green line). Predicted calculated z scores for the indicated signaling pathways are represented as being activated (UP) or downregulated (DOWN). **(B)** Heatmaps for differentially expressed NF-κB-dependent gene transcripts in patient vs. HD mDCs. **(C)** Human immune monitoring 65-Plex was used to analyze pro-inflammatory cytokines in cell-free supernatants harvested from HD (n=4) vs. melanoma patient (n=23) DCs. Error bars represent standard deviation. Patients were segregated based on clinical outcomes. CXCL9 and sCD40L inter-group differences were analyzed using one-way ANOVA analysis with Tukey's multiple comparison test, and TNFα and CXCL11 inter-group differences were analyzed using Kruskal-Wallis one-way ANOVA with Dunnett's multiple comparison test. **(D-E)** Validation

of the IPA analysis using Image Stream on HD DC p65 translocation into the nucleus vs. melanoma patients DCs post-maturation. Each end of the box and whisker plots represent the first (25%) and third (75%) quartile, while the middle line represents the mean. Patients were segregated based on clinical outcomes, with the significance of differences between cohorts determined using matched paired student t-tests (HD, D) or paired Wilcoxon rank sum test (patient data, E) . *p 0.05, **p 0.01, ***p 0.001, ns= not significant.
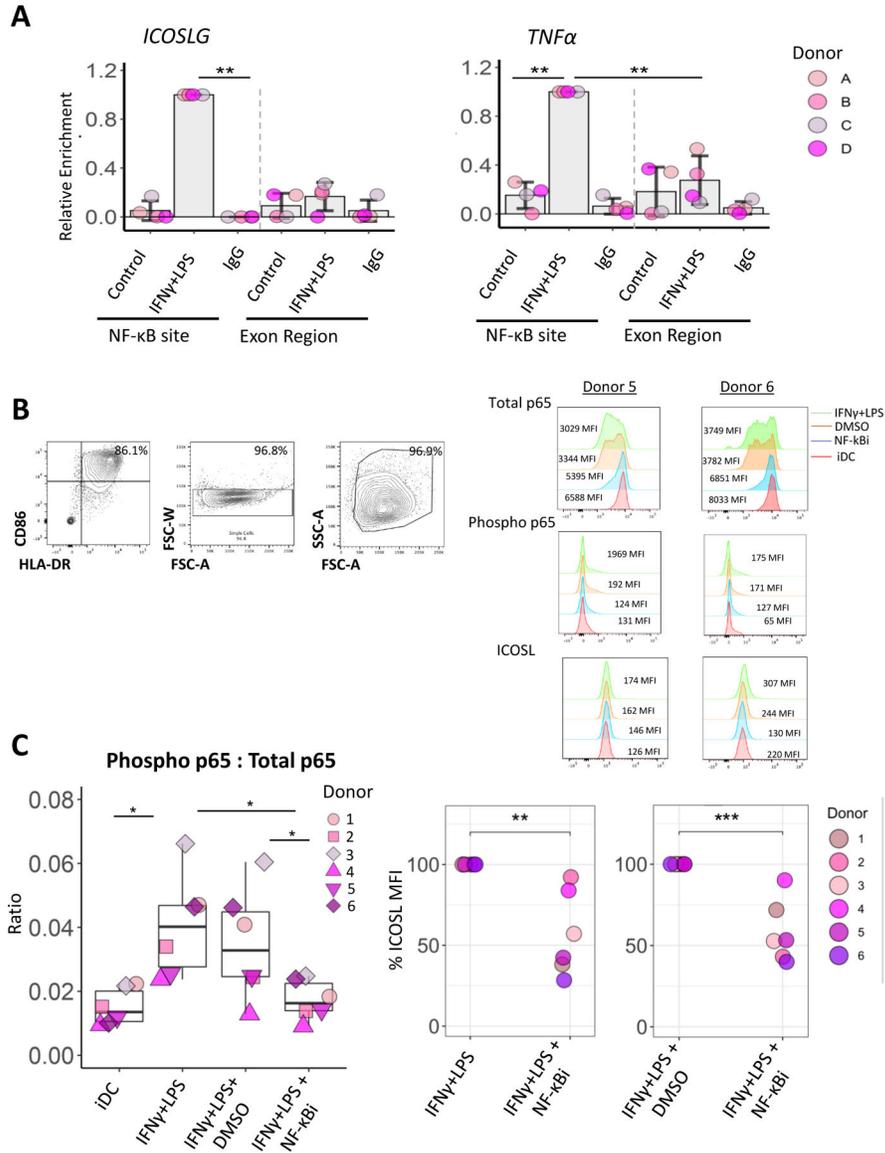
Figure 5. Canonical NF-κB signaling regulates ICOSL protein surface expression on human DCs.

(A) Chromatin immunoprecipitation assays performed on HD (n=4) cells to determine NF-κB p65 binding to the *ICOSLG* promoter region in IFNγ+LPS-treated (matured) DCs. TNFα was used as a positive control. Error bars represent standard deviation. The grey dotted line seperates the negative control experiments (Exon region) and the experimental group (NF-κB site) for *ICOSLG* and *TNFα* relative expression. **(B-C)** ICOSL surface expression analyzed from HD DCs (n=6) at baseline (day 5 iDCs), stimulated with IFNγ +LPS (15 minutes), IFNγ+LPS with DMSO (15 minutes), or IFNγ+LPS with the NFκB inhibitor, parthenolide (15 μM, 15 minutes). **(B)** Gating and histograms from two representative donors for total p65, phospho-p65, and ICOSL MFI values. Isotype antibodies were used to control for background staining. **(C)** The ratio of phospho-p65 to total p65 (left). ICOSL MFI values for each treatment group (right). Each end of the box and whisker plots represent the first (25%) and third (75%) quartile, while the middle line represents the

mean. Data is displayed as normalized percentages against the positive control (IFNγ+LPS) and unpaired student t-test (two-tailed) was used to determine significance. *p 0.05, **p 0.01.
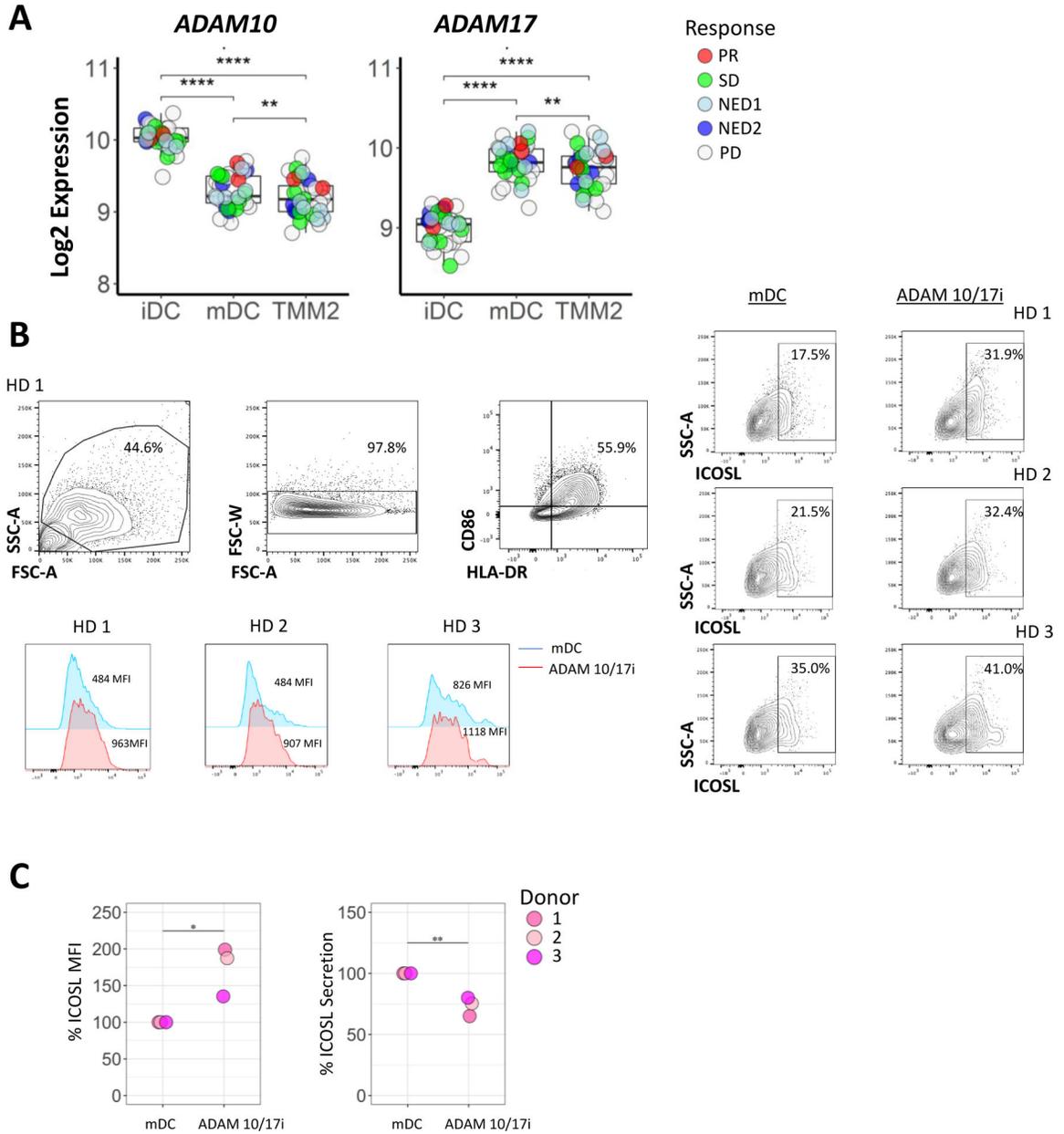
Figure 6. ICOSL is regulated, in part, by the metalloproteases, ADAM10 and ADAM17.
(A) Log2 mRNA expression of ADAM10 and ADAM17 for iDCs, mDCs, and AdV/DC in melanoma patients (n=33). Each end of the box and whisker plots represent the first (25%) and third (75%) quartile, while the middle line represents the mean. Patients were segregated by clinical outcomes, with intergroup significance determined using one-way ANOVA. **(B)** ICOSL surface expression analyzed from HD DCs (n=3) at baseline (iDCs), stimulated with IFNγ+LPS (24hrs.), or stimulated with IFNγ+LPS with the ADAM10/17 inhibitor, Tapi-2 (20 μM, 24hrs.). Gating is shown from a representative HD, and ICOSL frequencies and histograms are shown for mDC- and Tapi-2-treated cells. **(C)** ICOSL MFI or sICOSL for mDC controls and Tapi-2-treated cells. Data is displayed as normalized percentages against

the mDC control, and an unpaired student t-test (two-tailed) was used to determine significance. *p 0.05, **p 0.01, ***p 0.001.

Table 1.

sICOSL is a prognostic index for extended overall survival and progression-free survival of melanoma patients.

Univariate Cox regression analysis for sICOSL protein levels (n=15) or surface ICOSL MFI values (n=30) from baseline mDC culture supernatants or mDCs and AdV/DC, respectively. The hazard ratios, significance values, and 95% Confidence Intervals for OS and PFS are listed.

Endpoint	Factor	Cell Type	HR	95% CI for HR	p
OS	sICOSL	mDC	1	(0.082–0.81)	0.02
	ICOSL MFI	mDC	0.66	(0.30–1.47)	0.312
	ICOSL MFI	AdV/DC	1.72	(1.18–2.45)	0.00452

Endpoint	Factor	Cell Type	HR	95% CI for HR	p
PFS	sICOSL	mDC	1	(0.22–1.01)	0.053
	ICOSL MFI	mDC	1.33	(0.68–2.60)	0.409
	ICOSL MFI	AdV/DC	1.32	(0.96–1.81)	0.088